

## Coherent and incoherent multiple-harmonic generation from metal surfaces

A. T. Georges

*Department of Physics, University of Patras, Patras, 26110 Greece*

(Received 3 April 1996)

A theory is presented for multiple-harmonic generation from metal surfaces with the laser field polarized in the plane of incidence. The theory is applied to the analysis of a recent experiment on a gold surface. It is shown that the relatively slow decrease in the measured efficiency ( $10^{-10}$ – $10^{-13}$ ) for the second, third, fourth, and fifth harmonics is related to the stepwise nature of the excitation process. While for the second harmonic the intensities of the coherent and the incoherent component are comparable, for the higher harmonics the incoherent component dominates. [S1050-2947(96)04009-7]

PACS number(s): 42.65.Ky, 42.50.Hz

### I. INTRODUCTION

Optical second-harmonic generation (SHG) in reflection from a metal surface was one of the first nonlinear optical processes to be observed experimentally after the advent of the laser [1–3]. The energy conversion efficiency for this process is very small (less than  $10^{-9}$ ) because the thickness of the surface layer that can be excited at optical frequencies is only a few hundred angstroms. Despite this, SHG has important applications as a surface probe in laser studies of metal and semiconductor surfaces [3–5]. Recently, Farkas *et al.* reported the observation of multiple- (second-, third-, fourth-, and fifth-) harmonic generation (MHG) from a gold surface irradiated at a grazing angle with 35-psec, 5-GW/cm<sup>2</sup> pulses from a Nd:YAG (neodymium-doped yttrium aluminum garnet) laser [6]. The conversion efficiency for these four harmonics decreased very slowly ( $10^{-10}$ – $10^{-13}$ ) with increasing harmonic order. It was suggested that this feature is nonperturbative and similar to that observed in multiple odd-harmonic generation from noble gases under the influence of very intense ( $\sim 10^{15}$  W/cm<sup>2</sup>) laser fields, where in the case of Ne the conversion efficiency exhibits a plateau ( $10^{-9}$ – $10^{-11}$ ) from the 25th to the 135th harmonic [7]. However, the laser intensities used in the experiment on MHG from a gold surface are below the limit for breakdown of perturbation theory, and the measured dependence of the intensity of the four harmonics on the laser intensity is that predicted by perturbation theory. Hence, the two cases cannot have similar explanations. A recent theoretical paper on MHG from a metal surface based on the Sommerfeld model of a metal gives theoretical values in reasonable agreement with the experimental values for the relative efficiencies of the four harmonics [8]. But, it does not give any values for the absolute efficiencies, and does not account for energy relaxation and dephasing of the electronic states, which is essential for a correct description of the dynamics of any resonant optical process. Moreover, it does not account for reflection and refraction of the laser beam and the generated harmonics at the metal surface, and the inclusion of the appropriate harmonic-dependent Fresnel factors would change the predicted relative efficiencies.

In this paper we use the Sommerfeld model of a metal, extended to account phenomenologically for energy relaxation and dephasing of the electronic states due to electron-

phonon and electron-electron scattering, in order to study MHG from metal surfaces. As has been shown experimentally [6], the bulk contribution to MHG is very small compared to the surface contribution, and hence we can neglect it in our theory. The extended Sommerfeld model was used recently [9] to study the multiphoton surface photoelectric effect and gave good agreement with experiment [10]. The main finding in that work was that, due to the rapid dephasing of the electronic states, the multiphoton excitation of conduction electrons is a stepwise process. The stepwise nature of the excitation explains the comparable current densities that were observed in the one- and four-photon photoelectric effects on a gold surface at laser intensities of a few GW/cm<sup>2</sup>. As shown here, it explains also the relatively slow decrease in the intensity of the generated harmonics at the same laser intensities. While in previous studies of SHG from metal surfaces [1–3] the harmonic radiation is assumed to be purely coherent, it is shown here that in MHG from metal surfaces there are both coherent and incoherent components in the radiation field. The coherent component (elastic scattering) is associated with the average dipole of the oscillating electrons at the different harmonics, while the incoherent (inelastic scattering) is associated with the quantum fluctuations of these dipoles. For the second harmonic the two components are comparable, but for the higher harmonics the incoherent component dominates. In the case of a gaseous or bulk medium the incoherent component of the radiation would not be directional. As an example, consider third-harmonic generation (THG) in a gaseous medium under conditions of three-photon resonance and no intermediate resonance with an ideal monochromatic laser [11]. In addition to coherent THG codirectionally with the laser beam, there is also incoherent fluorescence from the three-photon excited state to the ground state, having the familiar doughnut-shaped radiation pattern of an oscillating electric dipole. In the case of a surface, however, because of boundary conditions for the fields, fluorescence from an  $N$ -photon excited state to the ground state is allowed only in the direction (within the limits of the uncertainty principle) of the reflected fundamental beam and the coherent harmonic radiation. The idea that narrow-band, incoherent harmonic radiation from a metal surface is directional should not seem strange. After all, white light from a flashlight retains its quasidirectionality upon reflection from a mirror. This is be-

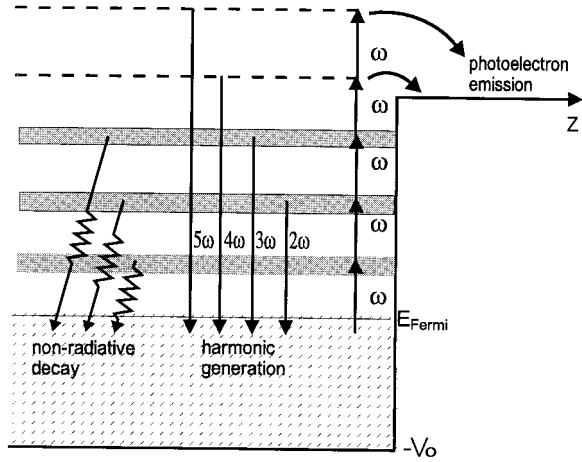


FIG. 1. Schematic diagram of the step potential at a metal surface and the processes that take place during laser-surface interaction.

cause the incident Gaussian stochastic field that is associated with white light, the induced stochastic linear polarization of the medium, and the reflected and refracted stochastic fields satisfy joint boundary conditions that lead to Snell's laws of linear reflection and refraction for stochastic fields. Note that in the case of MHG in reflection from a metal surface, the nonlinear surface polarizations that now play the role of the incident field are also Gaussian stochastic processes, because of the quantum nature of the elementary dipoles and the central limit theorem.

## II. THEORY

Figure 1 shows the basic processes of multiphoton absorption, nonradiative decay, photoelectron emission, and MHG that take place when a metal surface is irradiated with an intense laser beam. It is assumed that the laser intensity is below the critical value ( $\sim 10$  GW/cm<sup>2</sup> for picosecond pulses incident on a gold surface), above which thermionic emission and plasma formation at the surface become the dominant processes. The relative scaling for the photon energy and the work function of the metal corresponds to that in the recent experiment on a gold surface using a Nd:YAG laser [6]. The starting point of our theory for MHG is the familiar unperturbed energy eigenstates of an electron in a one-dimensional step potential,  $V(z) = -V_0$ ,  $z < 0$ , and  $V(z) = 0$ ,  $z > 0$  (outside the metal), which can be written in the form [8,9]

$$\phi(z) = \frac{1}{\sqrt{L_z}} \times \begin{cases} [e^{i\kappa_z z} + r e^{-i\kappa_z z}], & z < 0 \\ (1+r)e^{iq_z z}, & z > 0 \end{cases} \quad (1)$$

where  $L_z$  is a normalization length, and  $\kappa_z, q_z = (\kappa_z^2 - 2mV_0/\hbar^2)^{1/2}$  are the  $z$  components of the wave vector for the electron inside and outside the metal, respectively. The latter becomes purely imaginary ( $q_z = iq_z''$ ) for negative electron energies. The parameter  $r = (\kappa_z - q_z)/(\kappa_z + q_z)$  is the amplitude reflection coefficient. In the  $x$ - $y$  plane the electron is a free particle and its transverse momentum cannot change from the interaction with a laser field. Hence, in this

model, the laser-surface interaction reduces to a one-dimensional problem. The trouble with the plane-wave energy eigenstates given above is that they are not realistic for describing the motion of conduction electrons in the presence of electron-phonon and electron-electron scattering. Measurements of the transient reflectivity of a gold surface show that the energy relaxation rate for electrons 2 eV above the Fermi level is  $\gamma \approx 3 \times 10^{11}$  sec<sup>-1</sup> [12]. The dephasing (or momentum relaxation) rate accounts for both elastic and inelastic scattering, and is much greater than the energy relaxation rate. In the case of gold, matching the measured complex index of refraction [13] with the index of refraction for a free-electron gas with damping gives a momentum relaxation rate  $\Gamma \approx 5.5 \times 10^{15}$  sec<sup>-1</sup>, for photon energies in the range 2–10 eV. As a result of the dephasing, the energy eigenstates acquire an energy width equal to  $\hbar\Gamma$ , and this causes overlapping and mixing of the states within this energy range. Therefore, we consider normalized mixed states (wave packets) [9]

$$\Phi_i(z) = \frac{1}{\sqrt{\mathcal{N}_i}} \sum_{\alpha=1}^{\mathcal{N}_i} \sqrt{\mathcal{L}_{i,\alpha}} \phi_\alpha(z), \quad (2)$$

where  $\mathcal{L}_{i,\alpha} = (\Gamma_i/2)^2 / [\Delta\omega_\alpha^2 + (\Gamma_i/2)^2]$  are Lorentzian weights with  $\Delta\omega_\alpha$  being the frequency separation of the  $|\alpha\rangle$  state from the center frequency  $\omega_i$ ,  $\mathcal{N}_i = \pi g(\omega_i)\Gamma_i/2$  is the effective number of states within a Lorentzian line shape of width  $\Gamma_i$ , and  $g(\omega) = L_z m/2\pi\hbar\kappa_z$  the one-dimensional density of states for each spin state. The excitation of an electron by a laser beam proceeds resonantly through such mixed states, and the matrix element of the interaction Hamiltonian  $H'$  between two such states is

$$H'_{ij} \equiv \langle \Phi_i | H' | \Phi_j \rangle \approx \frac{\pi}{2} \sqrt{g(\omega_i)g(\omega_j)\Gamma_i\Gamma_j} \overline{H'}_{\alpha\beta}, \quad (3)$$

where  $\overline{H'}_{\alpha\beta}$  is the average matrix element over the  $\mathcal{N}_i\mathcal{N}_j$  pairs of unmixed states. It should be added that even during spontaneous emission an electron makes a transition between two mixed states.

Consider a laser beam of frequency  $\omega$  and electric field amplitude  $\mathcal{E}$  incident at a grazing angle  $\vartheta_i$  on a metal surface with the electric field linearly polarized in the plane of incidence ( $x$ - $z$  plane). In the plane-wave approximation, the  $z$  component of the electric field is

$$E_z(x, z, t) = \begin{cases} \mathcal{E} [e^{ik_z z} + \varrho e^{-ik_z z}] \sin\vartheta_i e^{i(\omega t - k_x x)} + \text{c.c.}, & z > 0 \\ \tau \mathcal{E}_0 e^{(ik'_{tz} + k''_{tz} z)} e^{i(\omega t - k_x x)} + \text{c.c.}, & z < 0, \end{cases} \quad (4)$$

where  $\varrho = (n \cos\vartheta_i - \cos\vartheta_r)/(n \cos\vartheta_i + \cos\vartheta_r)$  is the amplitude reflection coefficient, with  $n$  being the complex index of refraction of the metal, and  $\vartheta_r$  the complex angle of refraction.  $\mathcal{E}_0 = \mathcal{E}(1 + \varrho) \sin\vartheta_i$  is the amplitude at  $z = 0_+$ , and  $\tau = \epsilon_0/\epsilon(\omega)$  the ratio of the dielectric functions for the vacuum and the metal.  $k_x = (\omega/c) \sin\vartheta_i$ ,  $k_z = (\omega/c) \cos\vartheta_i$  are the components of the incident wave vector, and  $k'_{tz} = k'_{tz} - ik''_{tz} = (\omega/c) [\epsilon(\omega)/\epsilon_0 - \sin^2\vartheta_i]^{1/2}$  the complex  $z$  component of the wave vector in the metal. For the relative dielectric function  $\epsilon_r(\omega) = \epsilon(\omega)/\epsilon_0$  of the metal we use that

of a free-electron gas with damping,  $\epsilon_r(\omega) = 1 - \omega_p^2 / (\omega(\omega - i\Gamma))$ , with  $\omega_p$  being the plasma frequency. In the Coulomb gauge the interaction Hamiltonian is

$$\begin{aligned} H' &= -\frac{e}{2m} [A_z p_z + p_z A_z] \\ &= -\frac{e\hbar}{m\omega} \mathcal{E}_{z0} \left[ f(z) \frac{d}{dz} + \frac{1}{2} \frac{df(z)}{dz} \right] e^{i(\omega t - k_x x)} + \text{c.c.}, \end{aligned} \quad (5)$$

where  $p_z$  is the  $z$  component of the momentum operator, and  $A_z = -\int E_z dt$  the  $z$  component of the vector potential. Note that, since the excitation process is one-photon stepwise, we have neglected in the interaction Hamiltonian the term  $(e^2/2m)A^2$ , which is associated with two-photon absorption. The function  $f(z)$  gives the  $z$  dependence of the field, which in the interaction region can be approximated as

$$f(z) = \begin{cases} 1, & z > 0 \\ \tau e^{(ik'_{iz}z + k''_{iz}z)}, & z < 0 \end{cases} \quad (6)$$

where outside the metal we use the justifiable dipole approximation ( $e^{\pm ik_z z} \simeq 1$ ) for optical wavelengths, while inside we use the prescribed variation of the field. By allowing for variation of the vector potential inside the metal, the interaction Hamiltonian accounts not only for electric dipole but for higher-order multipoles as well.

The equation of motion for the slowly varying part,  $\sigma_{i,i+1}(t)$ , of the off-diagonal density matrix element  $\rho_{i,i+1} = \sigma_{i,i+1}(t) e^{i(\omega t - k_x x)}$  is [3,14]

$$\left[ \frac{d}{dt} + \frac{\Gamma_{i,i+1}}{2} \right] \sigma_{i,i+1} = \frac{i}{2} \Omega_{i,i+1} [\sigma_{i+1,i+1} - \sigma_{ii}], \quad (7)$$

where  $\sigma_{ii}$  is the fractional population of the electrons that have absorbed  $i$  photons, and on the right-hand side we have neglected higher-order terms associated with coupling to other mixed states.  $\Gamma_{i,i+1} = \Gamma_i + \Gamma_{i+1}$  is the transverse relaxation rate, and  $\Omega_{i,i+1} = 2\hbar^{-1} \tilde{\mu}_{i,i+1} \mathcal{E}_{z0}$  is the Rabi (interaction) frequency, with

$$\tilde{\mu}_{i,i+1} = \frac{e\hbar}{m\omega} \left\langle \Phi_i \left| f(z) \frac{d}{dz} + \frac{1}{2} \frac{df(z)}{dz} \right| \Phi_{i+1} \right\rangle \quad (8)$$

being a transition matrix element that accounts for electric dipole and higher-order multipoles of the surface states. In evaluating this matrix element, the second term, which is proportional to the  $z$  derivative of the field, can be neglected in comparison with the first term for  $z \neq 0$ , because the Fermi wave vector is much greater than the optical wave vector. At  $z = 0$ , the second term has a singularity due to the discontinuity of the normal field component at the surface, and this is taken into account in the calculations. Our calculations show that, in the case of the abrupt step surface potential model, the dominant contribution to the matrix elements of  $\tilde{\mu}$  comes from the first term in Eq. (8) and the part of the wave function inside the metal. We should point out here that, if we neglect the second term in Eq. (8), the matrix elements of  $\tilde{\mu}$  are equal to those of the effective electric dipole that was used in Ref. [9], where a  $\boldsymbol{\mu} \cdot \mathbf{E}$  interaction Hamiltonian was used with the electric field having an  $f(z)$  variation. For

times  $t \gg 1/\Gamma_{i,i+1}$  the derivative in Eq. (7) can be neglected, and the equation becomes  $\sigma_{i,i+1} = i\Omega_{i,i+1}(\sigma_{i+1,i+1} - \sigma_{ii}) / \Gamma_{i,i+1}$ . Using this relation we obtain the following rate equations for the populations  $\sigma_{ii}, i = 0, 1, \dots, N$ , in the case of  $N$ -photon excitation:

$$\frac{d}{dt} \sigma_{00} = R_{01}(\sigma_{11} - \sigma_{00}) + \gamma'_1 \sigma_{11} + \gamma'_2 \sigma_{22} + \dots + \gamma'_N \sigma_{NN}, \quad (9)$$

$$\begin{aligned} \frac{d}{dt} \sigma_{ii} &= R_{i-1,i}(\sigma_{i-1,i-1} - \sigma_{ii}) + R_{i,i+1}(\sigma_{i+1,i+1} - \sigma_{ii}) \\ &\quad - \gamma'_i \sigma_{ii} \quad \text{for } i < N, \end{aligned} \quad (10)$$

$$\frac{d}{dt} \sigma_{NN} = R_{N-1,N}(\sigma_{N-1,N-1} - \sigma_{NN}) - \gamma'_N \sigma_{NN}, \quad (11)$$

where  $R_{i,i+1} = |\Omega_{i,i+1}|^2 / \Gamma_{i,i+1}$  is the rate for the  $|i\rangle \leftrightarrow |i+1\rangle$  transition and  $\gamma'_i = \gamma_i + \gamma_{ee,i}$  the sum of the non-radiative energy decay rate and the electron emission rate from state  $|i\rangle$ . The spontaneous decay rate of the excited mixed states ( $\sim 10^6 \text{ sec}^{-1}$ ) is many orders of magnitude smaller than the nonradiative decay rate, and so we can neglect it in the calculation of the level populations. From the definitions of the probability current and the probability transmission coefficient it can be shown that the electron emission rate from state  $|i\rangle$  is given by

$$\gamma_{ee,i} = \frac{2}{\pi} \int_{\omega_{\text{th}}}^{\infty} \frac{\kappa_z q_z}{(\kappa_z + q_z)^2} \mathcal{L}_i(\omega) d\omega, \quad (12)$$

where  $\hbar \omega_{\text{th}} = V_0$  is the threshold energy for electron emission, and  $\mathcal{L}_i(\omega)$  the Lorentzian weight distribution that enters in Eq. (2). The electron emission rate from an above-threshold excited state increases rapidly with the number of photons absorbed above threshold, and the population of these states drops very rapidly. In numerical calculations the system of rate equations (9)–(11) can be truncated after the value of  $N$  for which the population of the  $N$ -photon excited state is negligible compared to that of the  $(N-1)$ -photon excited state. Note that since in the experiment the emitted electrons are replenished by the power supply of the circuit used to monitor electron emission simultaneously with MHG, in the rate equation for  $\sigma_{00}$  the emitted electrons are taken to return to the ground state.

In order to calculate the  $N$ th-order nonlinear surface polarization we need to know the off-diagonal density matrix element [3,14]  $\rho_{0N} = \sigma_{0N}(t) e^{iN(\omega t - k_x x)}$ . For times  $t \gg 1/\Gamma_{0N}$  the slowly varying part is given by

$$\sigma_{0N}(t) = -i \frac{1}{\Gamma_{0N}} [\sigma_{0,N-1} \Omega_{N-1,N} - \Omega_{01} \sigma_{1N}]. \quad (13)$$

In the case of  $N=2$  and  $N=3$  the equation above gives

$$\sigma_{02}(t) = -\frac{\Omega_{01} \Omega_{12}}{4\Gamma^2} [\sigma_{00} - 2\sigma_{11} + \sigma_{22}], \quad (14)$$

and

$$\sigma_{03}(t) = i \frac{\Omega_{01}\Omega_{12}\Omega_{23}}{8\Gamma^3} [\sigma_{00} - 3\sigma_{11} + 3\sigma_{22} - \sigma_{33}], \quad (15)$$

where in order to simplify the two expressions we have set all the  $\Gamma_{ij}$ 's appearing in them equal to  $2\Gamma$ . From the last two equations we see that  $\sigma_{0N} \propto (\Omega/\Gamma)^N$ , where  $(\Omega/\Gamma) \ll 1$  for laser intensities below the damage limit of the surface. Hence, the off-diagonal density matrix elements are much smaller than the diagonal ones, and they decrease rapidly with increasing  $N$ . This shows that the multiphoton excitation of conduction electrons is incoherent.

### A. Nonlinear surface polarizations

Since the thickness of the surface layer that is excited by the laser field is much less than the wavelength of the harmonics that it generates, we can treat the polarized layer as a polarization sheet at  $z=0$ . The quantum operator for the nonlinear surface polarization at the  $N$ th harmonic can then be written as

$$\hat{P}_{Ns_z} = \hat{\mathcal{P}}_{Ns_z}(t) e^{iN(\omega t - k_x x)} + \text{H.c.}, \quad (16)$$

where

$$\hat{\mathcal{P}}_{Ns_z}(t) = \frac{d}{V} \sum_i \hat{\sigma}_{0N,i}(t) \tilde{\mu}_{N0,i} \quad (17)$$

is the quantum amplitude of the surface polarization, with  $d = 1/k_{tz}''$  being the optical skin depth of the metal, and  $V$  the volume of the excited surface layer. The sum is over the initial electron states, and it is used here symbolically instead of the more complicated integral over the Fermi sphere, which we use in the final results below. The operator  $\hat{\sigma}_{0N}$  and its Hermitian conjugate  $\hat{\sigma}_{N0}$  are electron lowering and raising operators, respectively, and their expectation values are the density matrix elements  $\sigma_{0N}$  and  $\sigma_{N0}$ , which are given by Eq. (13) and its complex conjugate. The expression for the nonlinear surface polarization is consistent with the interaction Hamiltonian, and represents a generalized electric polarization that accounts for electric dipole and higher-order multipoles. Unlike previous theories of SHG from metal surfaces [2,3], where the nonlinear polarization is described in terms of a constant susceptibility, with the implicit weak-field assumption that the populations of the excited electronic states are zero, the present theory can account for strong electron excitation as in the case of the recent experiment on MHG [6]. Our calculations for this case show that at a laser intensity of  $5 \text{ GW/cm}^2$  about 20% of the electrons with initial energy near the Fermi energy are in excited states. In this respect, MHG from metal surfaces has some common aspects with resonant harmonic generation from metal vapors under strong laser fields, which also cannot be described in terms of a constant nonlinear susceptibility [14].

The nonlinear surface polarization at  $N\omega$  gives rise to reflected and transmitted harmonic waves with electric field operators

$$\hat{\mathbf{E}}_{Nr}(x, z, t) = \hat{\mathcal{E}}_{Nr}(t) \exp[i(N\omega t - k_{Nrx}x - k_{Nrz}z)] + \text{H.c.}, \quad (18)$$

$$\hat{\mathbf{E}}_{Nt}(x, z, t) = \hat{\mathcal{E}}_{Nt}(t) \exp[i(N\omega t - k_{Ntx}x + k_{Ntz}z)] + \text{H.c.}, \quad (19)$$

where  $k_{Nrx} = (N\omega/c) \sin \vartheta_r$ ,  $k_{Nrz} = (N\omega/c) \cos \vartheta_r$  are the wave-vector components of the reflected harmonic wave, and  $k_{Ntx}$ ,  $k_{Ntz} = k'_{Ntz} - ik''_{Ntz}$  those of the transmitted wave. Note that our treatment of the harmonic fields as quantum operators has to do with the quantum properties of the electronic polarization, and not with quantization of the field energy. The latter is not necessary in the theoretical treatment of this problem. In the case of a  $z$ -polarized dipole sheet at  $z=0$ , the reflected and transmitted waves must satisfy the boundary conditions [3,15]

$$\hat{\mathbf{E}}_{Nrx} - \hat{\mathbf{E}}_{Ntx} = \frac{1}{\epsilon(N\omega)} \frac{\partial \hat{\mathcal{P}}_{Ns_z}}{\partial x}, \quad (20)$$

and

$$\mathbf{k}_{Nr} \times \hat{\mathbf{E}}_{Nr} = \mathbf{k}_{Nt} \times \hat{\mathbf{E}}_{Nt}. \quad (21)$$

In order for the two conditions to be satisfied for every  $x$ , the fast varying propagation factors in the expressions for the nonlinear polarization and the two fields must be equal, and hence it follows that  $k_{Nrx} = k_{Ntx} = Nk_x$ . Therefore, in the plane-wave approximation, the angle of reflection for the harmonic wave is equal to the angle of incidence of the fundamental wave. This is true for both the coherent and the incoherent components of the reflected harmonic fields. From Eqs. (20) and (21), we can then show that the quantum operator for the amplitude of the electric field of the reflected  $N$ th harmonic is given by

$$\hat{\mathcal{E}}_{Nr} = i \frac{N\omega F}{c\epsilon(N\omega)} \hat{\mathcal{P}}_{Ns_z}, \quad (22)$$

where  $F = n_{N\omega} \sin \vartheta_i / (n_{N\omega} \cos \vartheta_i + \cos \vartheta_{Nr})$  is a Fresnel coefficient for the  $N$ th harmonic, with  $n_{N\omega} = [\epsilon_r(N\omega)]^{1/2}$  being the index of refraction of the metal at  $N\omega$ , and  $\vartheta_{Nt}$  the angle of refraction for the transmitted  $N$ th harmonic. The reflected harmonic fields are polarized in the plane of incidence, and have the same polarization as the reflected fundamental field, in agreement with experimental observations [6]. It should be noted that the coherent component of the  $N$ th harmonic field, which is given by the expectation value of Eq. (22), follows the phase of the  $N$ th power of the incident field amplitude since  $\langle \hat{\mathcal{P}}_{Ns_z} \rangle \propto \sigma_{0N} \propto \mathcal{E}^N$  [see Eqs. (14) and (15)]. The incoherent component  $\delta \hat{\mathcal{E}}_{Nr} = (\hat{\mathcal{E}}_{Nr} - \langle \hat{\mathcal{E}}_{Nr} \rangle) \propto (\hat{\sigma}_{0N} - \sigma_{0N})$ , however, does not follow the phase of the incident field because of quantum fluctuations, which in a Langevin approach are accounted for by an additive noise source term in the equation of motion for  $\hat{\sigma}_{0N}$  [16].

### B. Intensity of coherent and incoherent harmonic radiation

The intensity of the coherent (elastic) component of the reflected  $N$ th harmonic is given by

$$I_{\text{coh}}(N\omega) = 2c\epsilon_0 \frac{(N\omega)^2 |F|^2}{c^2 |\epsilon(N\omega)|^2} |\langle \hat{\mathcal{P}}_{Nsz} \rangle|^2, \quad (23)$$

where

$$\langle \hat{\mathcal{P}}_{Nsz} \rangle = d \frac{1}{4\pi^3} \int d\Omega_{\kappa_i} \int (\sigma_{0N} \tilde{\mu}_{N0})_{\kappa_i, \theta_i} P_{\text{FD}}(\kappa_i) \kappa_i^2 d\kappa_i \quad (24)$$

is the expectation value of the surface polarization. The integration is over the Fermi sphere, with  $\kappa_i, \theta_i$  being the initial electron wave number and angle from the  $z$  axis.  $P_{\text{FD}}(\kappa_i)$  is the Fermi-Dirac probability distribution, and the two spin states are taken into account. It should be pointed out here that, in nonlinear optics [3], the general rule is to consider only the coherent radiation that is emitted by the average polarization. However, in MHG from metal surfaces we must also consider the incoherent radiation that is emitted by the fluctuations in the polarization,  $\delta \hat{\mathcal{P}}_{Nsz} = \hat{\mathcal{P}}_{Nsz} - \langle \hat{\mathcal{P}}_{Nsz} \rangle$ , and which turns out to be more intense than the coherent radiation. To our knowledge, the treatment of the incoherent radiation in MHG from metal surfaces that is presented below is the first such treatment.

The total average intensity of the reflected  $N$ th harmonic,  $I_{\text{tot}}(N\omega) = I_{\text{coh}}(N\omega) + I_{\text{inc}}(N\omega)$ , with  $I_{\text{inc}}(N\omega)$  being the average intensity of the incoherent component, is given, as in the case of resonance fluorescence [16], by

$$I_{\text{tot}}(N\omega) = 2c\epsilon_0 \frac{(N\omega)^2 |F|^2}{c^2 |\epsilon(N\omega)|^2} \langle \hat{\mathcal{P}}_{Nsz}^\dagger \hat{\mathcal{P}}_{Nsz} \rangle, \quad (25)$$

where

$$\begin{aligned} \langle \hat{\mathcal{P}}_{Nsz}^\dagger \hat{\mathcal{P}}_{Nsz} \rangle &= \frac{d^2}{V^2} \sum_{i,f} \langle \hat{\sigma}_{N0,i} \hat{\sigma}_{0N,f} \rangle \tilde{\mu}_{0N,i} \tilde{\mu}_{N0,f} \\ &= \frac{d}{A} \left[ \frac{1}{V} \sum_i \sigma_{NN,i} \left| \tilde{\mu}_{N0,i} \right|^2 \right], \end{aligned} \quad (26)$$

with  $A = V/d$  being the excited surface area. If we now express  $|\tilde{\mu}_{N0,i}|^2$  in terms of the spontaneous decay rate of state  $|N\rangle$ ,

$$\gamma_{\text{sp},N} = \frac{(N\omega)^3 |\tilde{\mu}_{N0,i}|^2}{8\pi^2 \epsilon_0 c^3 \hbar} \Delta\Omega_k, \quad (27)$$

where  $\Delta\Omega_k$  is the small solid angle of the spontaneous emission cone with axis a classical reflected ray, Eq. (25) becomes

$$I_{\text{tot}}(N\omega) = Rd \frac{|F|^2}{|\epsilon_r(N\omega)|^2} \hbar N\omega \langle \gamma_{\text{sp},N} \sigma_{NN} \rangle, \quad (28)$$

where

$$\begin{aligned} \langle \gamma_{\text{sp},N} \sigma_{NN} \rangle &= \frac{1}{4\pi^3} \int d\Omega_{\kappa_i} \int (\gamma_{\text{sp},N} \sigma_{NN})_{\kappa_i, \theta_i} \\ &\quad \times [1 - P_{\text{FD}}(\kappa_i)] P_{\text{FD}}(\kappa_i) \kappa_i^2 d\kappa_i \end{aligned} \quad (29)$$

is the average number of harmonic photons emitted per unit volume per unit time. The factor  $[1 - P_{\text{FD}}(\kappa_i)]$  is the prob-

ability that the final state is not occupied. The parameter  $R = (4\lambda_N^2/A)/\Delta\Omega_k$ , with  $\lambda_N$  being the wavelength of the  $N$ th harmonic, is the ratio of the diffraction solid angle in the case of a rectangular aperture of area  $A$  and the spontaneous emission solid angle  $\Delta\Omega_k$ . In this work, it is assumed that spontaneous emission at a metal surface is diffraction limited, and  $R$  is set equal to unity. The final expression for  $I_{\text{tot}}(N\omega)$ , which is derived using the quantum properties of the nonlinear polarization, is exactly what one would have obtained on the basis of a simple energy analysis. That is,  $I_{\text{tot}}(N\omega)$  is equal to the number of electrons per unit volume that have absorbed  $N$  photons, times the spontaneous decay rate, times the photon energy, times the fraction  $|F/\epsilon_r(N\omega)|^2$  that is emitted from the surface layer to the vacuum, times the thickness of the layer. Before closing this section, it should be emphasized that harmonic generation is a spontaneous process with respect to the emitted harmonic photons, and the main difference between the coherent and the incoherent components is in the spectrum and the photon statistics. For a monochromatic laser field, the coherent component of the generated harmonics is monochromatic and has Poisson photon statistics. The incoherent component, on the other hand, has a spectral width of the order of  $4k_B T \approx 0.1$  eV at room temperature [8], while its photon statistics are Gaussian. It should be mentioned here that the authors of Ref. [8] treat MHG as a spontaneous process and calculate the emission rates for the harmonic photons using Fermi's golden rule, instead of the nonlinear polarizations as we do here. In their treatment they do not distinguish between coherent and incoherent components of the generated harmonics, and do not account for the directional properties of MHG from metal surfaces.

### III. DISCUSSION OF NUMERICAL RESULTS

Calculations have been carried out using parameters corresponding to those in the recent experiment on MHG from a gold surface with a Nd:YAG laser of wavelength  $\lambda = 1.06$   $\mu\text{m}$ . The parameters that have been used for gold are as follows: Fermi energy = 5.51 eV,  $V_0 = 10.19$  eV (work function of 4.68 eV) [6,10],  $\omega_p = 1.37 \times 10^{16}$  rad/sec,  $\gamma = 3 \times 10^{11}$  sec $^{-1}$ , and  $\Gamma = 5.5 \times 10^{15}$  sec $^{-1}$ . The temperature in the Fermi-Dirac distribution was set equal to 300 K. In the calculations for this case, the system of rate equations (9)–(11) was truncated after  $N=6$ , as the calculated intensity of the sixth harmonic is four orders of magnitude lower than that of the fifth harmonic, and the former was not detected in the experiment.

Figure 2 shows the theoretical dependence of the total intensity of the second, third, fourth, and fifth harmonic, and the intensity of the coherent component of the second and third harmonic on the laser intensity in the range between  $10^8$  and  $6 \times 10^9$  W/cm $^2$ , with the angle of incidence equal to  $70^\circ$ . For higher laser intensities, experiments show that temperature effects, thermionic emission, and plasma formation become important [10], and then our theoretical analysis is not valid. The first thing we note is that for laser intensities below 1 GW/cm $^2$ , the intensity of the harmonics varies as  $I(N\omega) \propto I^N(\omega)$ , in agreement with perturbation theory and the experiment. For higher laser intensities, the slope of the curves decreases slowly due to strong electron emission,

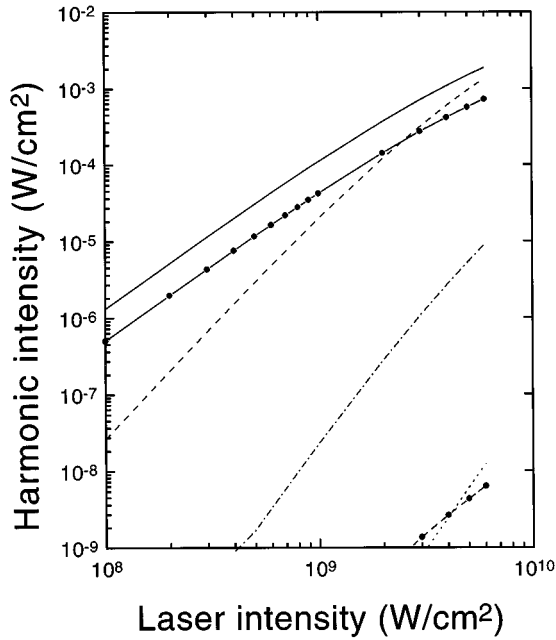


FIG. 2. Plot of the total intensity of the reflected second (solid line), third (dashed line), fourth (dot-dash line), and fifth (dotted line) harmonic vs the laser intensity with the angle of incidence equal to  $70^\circ$ . Also plotted is the intensity of the coherent component of the second (solid line with points) and the third (dashed line with points) harmonic.

which competes with harmonic generation. In the case of the second harmonic, the intensity of the coherent component is about  $1/3$  of the total intensity, while in the case of the third harmonic the corresponding fraction is only  $10^{-5}$ . For the higher harmonics the intensity of the coherent component relative to the total intensity is even more negligible. As we pointed out earlier, this is due to the rapid dephasing and the vanishing coherence of the excited states of conduction electrons. The absolute conversion efficiency for the second harmonic at  $5 \text{ GW/cm}^2$  is about two orders of magnitude smaller than the experimental value of  $\sim 10^{-10}$  [6]. This must be attributed to the fact that, as has been shown by calculations of SHG from metal surfaces using the density-functional approach [17], the abrupt step surface potential model underestimates the nonlinear polarizability of real metal surfaces. Despite this shortcoming, the Sommerfeld model of a metal surface allows us to examine other important aspects of the nonlinear optical process of MHG from metal surfaces. The calculated ratios of the relative efficiencies  $I_{\text{tot}}(N\omega)/I_{\text{tot}}(2\omega)$ , for  $N=2, \dots, 5$  at  $5 \text{ GW/cm}^2$  are equal to 1,  $6.3 \times 10^{-1}$ ,  $3.6 \times 10^{-3}$ , and  $0.4 \times 10^{-5}$ . For the first three harmonics these values agree very well with the experimental values, 1,  $5 \times 10^{-1}$ ,  $5 \times 10^{-3}$ , and  $1 \times 10^{-3}$ . The slow decrease in the intensity of the first three harmonics reflects the slow decrease in the electron populations that have absorbed 2, 3, and 4 photons, respectively. The latter is due to the stepwise nature of the excitation of conduction electrons [9]. For the fifth harmonic the theoretical value for the relative efficiency is about two orders of magnitude lower than the experimental value. In the context of our independent particle theory of MHG, which accounts only for single-particle excitation, the low efficiency for the fifth har-

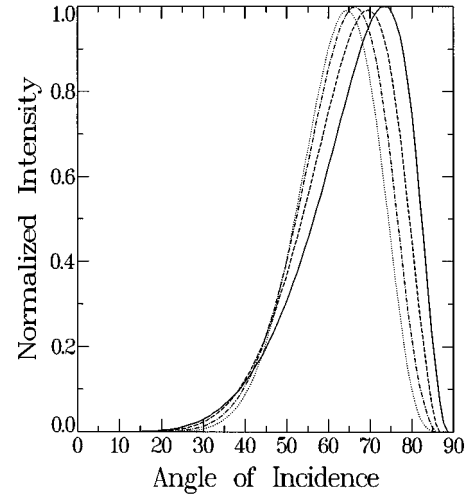


FIG. 3. Plot of the total intensity of the reflected second (solid line), third (dashed line), fourth (dot-dash line), and fifth (dotted line) harmonic vs the angle of incidence (in degrees) at a laser intensity of  $5 \text{ GW/cm}^2$ .

monic is caused by the competing process of above-threshold electron emission (see Fig. 1). The experimental observation that the fifth harmonic is *only* five times weaker than the fourth, *while the fourth harmonic is 100 times weaker than the third*, must be attributed to an enhancement from a collective excitation of the conduction electrons, which is not accounted for in the present theory. Such an enhancement has been predicted in the case of SHG in calculations using the density-functional approach for  $2\omega$  near  $0.8\omega_p$ , and is due to excitation of electron-hole pairs in the surface region [17]. We should also note that the energy of the fifth-harmonic photons ( $5\hbar\omega = 5.85 \text{ eV}$ ) is close to the energy of surface plasmons in gold ( $\hbar\omega_p/\sqrt{2} = 6.36 \text{ eV}$ ), and it is possible that this plays a role in the case of the fifth harmonic.

Figure 3 shows the theoretical dependence of the total intensity of the first four harmonics on the angle of incidence  $\vartheta_i$ , at a laser intensity of  $5 \text{ GW/cm}^2$ . The four angle tuning curves are similar, and the main difference is that the angle at which the intensity is maximum decreases from about  $73^\circ$ , in the case of the second harmonic, to about  $65^\circ$ , in the case of the fifth harmonic. While the experiment did not examine this detail, the theoretical prediction for maximum efficiency in the neighborhood of  $\vartheta_i = 70^\circ$  is in good agreement with the experiment. The full width at half maximum of the angle tuning curves decreases from about  $26^\circ$ , in the case of the second harmonic, to about  $23^\circ$ , in the case of the fifth harmonic.

In conclusion, we have presented a theory of MHG from metal surfaces based on an extension of the Sommerfeld model for conduction electrons. We have explained the basic physics of this nonlinear optical process, and pointed out the incoherent nature of the higher harmonics. Since MHG probes more and higher excited states of conduction electrons than SHG by itself, the theoretical and experimental study of this multiple process can provide more information about surface states and electron dynamics than SHG.

## ACKNOWLEDGMENTS

The author gratefully acknowledges useful discussions with C. Fotakis, S. D. Moustazis, and N. A. Papadogiannis

regarding their experimental results. He also thanks the Institute of Electronic Structure and Laser in Crete, Greece, for its hospitality during his stay there when part of this work was carried out.

- 
- [1] F. Brown, R. E. Parks, and A. M. Sleeper, *Phys. Rev. Lett.* **14**, 1029 (1965).
  - [2] N. Bloembergen, R. K. Chang, S. S. Jha, and C. H. Lee, *Phys. Rev.* **174**, 813 (1968).
  - [3] Y. R. Shen, *The Principles of Nonlinear Optics* (Wiley, New York, 1984).
  - [4] S. A. Akhmanov, N. I. Koroteev, G. A. Paitian, I. L. Shumay, M. F. Galjautdinov, I. B. Khaibullin, E. I. Shtyrkov, *J. Opt. Soc. Am. B* **2**, 283 (1985).
  - [5] Y. R. Shen, *Nature* **337**, 519 (1989).
  - [6] Gy. Farkas, Cs. Toth, S. D. Moustazis, N. A. Papadogiannis, and C. Fotakis, *Phys. Rev. A* **46**, R3605 (1992).
  - [7] A. L'Huillier and Ph. Balcou, *Phys. Rev. Lett.* **70**, 774 (1993).
  - [8] S. Varro and F. Ehlitzky, *Phys. Rev. A* **49**, 3106 (1994).
  - [9] A. T. Georges, *Phys. Rev. B* **51**, 13 735 (1995).
  - [10] S. D. Moustazis, M. Tatarakis, C. Kalpouzos, and C. Fotakis, *Appl. Phys. Lett.* **60**, 1939 (1992).
  - [11] J. C. Miller, R. N. Compton, M. G. Payne, and W. W. Garrett, *Phys. Rev. Lett.* **45**, 114 (1980).
  - [12] R. W. Schoenlein, W. Z. Lin, J. G. Fujimoto, and G. L. Eesley, *Phys. Rev. Lett.* **58**, 1680 (1987).
  - [13] J. H. Weaver, C. Krafka, D. N. Lynch, and E. E. Koch, *Optical Properties of Metals* (Fach-Inform-Zentrum, Karlsruhe, 1981).
  - [14] A. T. Georges, P. Lambropoulos, and J. H. Marburger, *Phys. Rev. A* **15**, 300 (1977).
  - [15] T. F. Heinz, in *Nonlinear Surface Electromagnetic Phenomena*, edited by H.-E. Ponath and G. I. Stegeman (Elsevier, Amsterdam, 1991), Chap. 5, p. 353.
  - [16] C. Cohen-Tannoudji, J. Dupont, and G. Grynberg, *Atom-Photon Interactions* (Wiley, New York, 1991), pp. 379–387.
  - [17] A. Liebsch and W. L. Schaich, *Phys. Rev. B* **40**, 5401 (1989).